MOFFAT, K., SZEBENYI, D. & BILDERBACK, D. (1984). *Science*, **233**, 1423–1425.
PIANETTA, P. & BARBEE, T. W. (1988). *Nucl. Instrum. Methods*, **A266**, 441–446.
VICCARO, P. J. & SHENOY, G. K. (1988). *Nucl. Instrum. Methods*, **A266**, 112–115.
ZACHARIASEN, W. H. (1945). *Theory of X-ray Diffraction in Crystals*. New York: Wiley.

Acta Cryst. (1989). A**45**, 726–732

Genera of Minimal Balance Surfaces

BY WERNER FISCHER AND ELKE KOCH

Institut für Mineralogie der Universität Marburg, Hans-Meerwein-Strasse, D-3550 Marburg, Federal Republic of Germany

(*Received* 7 *April* 1989; *accepted* 1 *June* 1989)

Abstract

The genus of a three-periodic intersection-free surface in R^3 refers to a primitive unit cell of its symmetry group. Two procedures for the calculation of the genus are described: (1) by means of labyrinth graphs; (2) *via* the Euler characteristic derived from a tiling on the surface. In both cases new formulae based on crystallographic concepts are given. For all known minimal balance surfaces the genera and the labyrinth graphs are tabulated.

1. Introduction

In a series of papers (Fischer & Koch 1987; 1989*a*, *b*; Koch & Fischer 1988, 1989*a*, *b*) minimal balance surfaces, *i.e.* three-periodic minimal surfaces subdividing R^3 into two congruent labyrinths, have been studied with respect to their symmetry properties. It turns out that the symmetry of a minimal balance surface is best described by a pair of space groups G–H, where G represents the full symmetry of the surface and H is that subgroup of G with index 2 that does not interchange the two labyrinths and the two sides of the surface. Instead of space-group pairs proper black–white space groups may also be used (*cf.* Mackay & Klinowski, 1986; Fischer & Koch, 1987). New types of minimal balance surfaces have been derived making use of the fact that each twofold axis belonging to G but not to H has to lie within each minimal balance surface with symmetry G–H.

Within the cited papers for each minimal balance surface the fundamental topological constant called the genus has been given without an explanation of how it had been calculated. This will be given below.

2. The genus of a minimal balance surface

A non-periodic surface in R^3 is said to be of *genus* g, if it may topologically be deformed to a sphere with g handles. According to this definition an ellipsoid and also a plane have genus 0, a torus (doughnut with one hole) genus 1, a pretzel (doughnut with two holes) genus 2 *etc.* Consequently, each three-periodic minimal surface has an infinite genus in this sense.

Therefore, a modified definition has been introduced for the genus of a three-periodic minimal surface (Schoen, 1970) counting only the number of handles per unit cell. In other words, the surface is embedded in a (flat) three-torus T^3 to get rid of all translations, and then the conventional definition of the genus is applied. The procedure of constructing T^3 from R^3 corresponds to identifying the opposite faces of the primitive unit cell [for a popular introduction to such manifolds see Weeks (1985)]. This may be visualized in analogy to transferring a two-periodic pattern in R^2 to the torus T^2 by rolling up a two-dimensional unit cell in both directions. In this approach an object moving within one labyrinth of the minimal surface and leaving the unit cell across one face will reenter it through the translationally equivalent opening on the opposite face. Obviously, the unit cell used has to refer to H, because otherwise the moving object thereby might change into the other labyrinth.

The genus of a three-periodic minimal surface may be calculated in different ways, two of which will be discussed here: (1) by means of the labyrinth graphs (Schoen, 1970; Hyde, 1989); (2) *via* the Euler characteristic determined with the aid of any tiling on the surface.

A third possibility makes use of the flat points of the surface (Hyde, 1989). As flat points are not easily discernible in all cases, however, it seems more appropriate to facilitate the search for flat points by the knowledge of the genus.

3. Labyrinth graphs

As a three-periodic minimal surface without self-intersection and the labyrinths separated by it are

0108-7673/89/100726-07$03.00

complex objects, Schoen (1970) proposed to represent each labyrinth by a graph (skeletal graph in his terminology). The connectedness of a labyrinth and the interpenetration with its counterpart may be visualized more easily from the two graphs.

For each of the two labyrinths associated with an intersection-free three-periodic minimal surface a *labyrinth graph* may be constructed as follows. Each graph is entirely located within its labyrinth; each branch of a labyrinth contains an edge of its graph; each circuit of one labyrinth graph encircles an edge of the other one.

Any of the two labyrinth graphs may be used to represent the surface. As each circuit of the graph corresponds to a handle of the surface, the number of circuits per unit cell (with respect to H in the case of a minimal balance surface) or of the finite graph embedded in T^3 has to be counted to get the genus. This may be done in two different ways.

(*a*) In a modification of the procedure proposed by Hyde (1989) a connected subgraph containing no translationally equivalent vertices may be separated from one labyrinth graph. Then

$$g = p/2 + q \qquad (1)$$

holds, where p is the number of edges connecting the finite subgraph to the rest of the infinite labyrinth graph and q means the number of edges that must be omitted to make the subgraph simply connected. As p equals at least 6 the genus of a three-periodic surface without self-intersection must be $g \geq 3$.

(*b*) Keeping in mind the embedding in the flat torus T^3, we may derive a more crystallographic formula. The number of edges in the embedded labyrinth graph may be calculated from

$$e = \sum_i m_i e_i/2,$$

where m_i is the multiplicity of the ith vertex with respect to a primitive unit cell of H, e_i is the number of edges meeting at this vertex and i runs over all symmetrically inequivalent vertices of the labyrinth graph. Then g is the difference between e and the number e_s of edges in any simply connected subgraph with the same number v of vertices. As

$$e_s = v - 1 = \sum_i m_i - 1$$

holds, it follows that

$$g = 1 + \sum_i m_i(e_i/2 - 1). \qquad (2)$$

As labyrinth graphs may help to visualize minimal balance surfaces, details of labyrinth graphs are given in Table 1. Each type of minimal balance surface is characterized by its symbol in column 1, its inherent symmetry G–H in column 2 and the reference number of its pattern of twofold axes (linear skeletal net) in column 3 (Fischer & Koch 1987, 1989*a*, *b*; Koch & Fischer, 1988, 1989*a*, *b*). The genus is given in column 4. The last three columns contain information on one of the two labyrinth graphs. In column 5 its vertices are described by their Wyckoff letters, their site symmetries and a reference point for each kind. The adjacent vertices of each reference point, *i.e.* the vertices connected to it by edges of the graph, are indicated in column 6. For this, each set of adjacent vertices, which are equivalent with respect to the site symmetry of the reference point, is represented by only one coordinate triplet followed by the number of such vertices in parentheses. If vertices are not completely fixed by symmetry suitable values for the free parameters are given in the last column.

A closer inspection of the table reveals a remarkable property of different minimal balance surfaces spanned by the same set of plane nets of twofold axes: in most cases the genus is the same for minimal balance surfaces consisting of either catenoids, multiple catenoids, infinite strips or branched catenoids. The reason for this is displayed in their labyrinth graphs. In a minimal balance surface with catenoid-like surface patches two adjacent catenoids between the same pair of nets are centred by vertical edges of the same labyrinth graph and separated by a channel of the second labyrinth containing a horizontal edge of the second graph. If these two catenoids are united to a multiple catenoid this edge of the second graph is removed and a new horizontal edge connecting the two centres of the catenoids is added to the first graph. As both graphs are congruent this procedure amounts to shifting part of the edges within each labyrinth graph. As the sum in (2) is unchanged, this shifting of edges does not change the genus as long as the unit cell is preserved. An example is given in Fig. 1.

If, however, shifting of edges changes the symmetry such that the unit cell is not retained, the genus also changes. Formula (2) shows that an enlargement of the unit cell by a factor of n results in a change of g into

$$g_n = 1 + n(g - 1) \qquad (3)$$

[*cf.* also (6) and (9) to (12) below]. Accordingly a *tP* surface has genus 3, whereas – owing to the doubling of the primitive unit cell of *Cmmm* compared with that of *P4/mmm* – the genus of an *MC*5 surface is 5. Formula (3) also holds if one and the same minimal balance surface is described not only in the smallest possible unit cell but also in a multiple cell. The genus of a minimal balance surface as defined above, therefore, only makes sense if it is referred to its inherent symmetry.

4. Euler characteristics

An intersection-free surface in R^3 (or T^3) may also be characterized by a number χ, called its *Euler characteristic*. χ is related to the genus of the surface

Table 1. *The genera and the labyrinth graphs for all known minimal balance surfaces.*

Minimal surface	G-H	Case	Genus	Labyrinth graph in H		
				Vertices	Adjacent vertices	Parameters
P	$Im\bar{3}m$-$Pm\bar{3}m$	1	3	1*a* $m\bar{3}m$ 000	100(6)	
$C(P)$	$Im\bar{3}m$-$Pm\bar{3}m$	1	9	1*a* $m\bar{3}$m 000	$0\frac{1}{2}\frac{1}{2}$(12)	
				3*c* 4/*mm.m* $0\frac{1}{2}\frac{1}{2}$	000(4)	
D	$Pn\bar{3}m$-$Fd\bar{3}m$	2	3	8*a* $\bar{4}3m$ 000	$\frac{1}{4}\frac{1}{4}\frac{1}{4}$(4)	
$C(D)$	$Pn\bar{3}m$-$Fd\bar{3}m$	2	19	8*a* $\bar{4}3m$ 000	$\frac{1}{8}\frac{1}{8}\frac{\bar{3}}{8}$(12)	
				16*d* .$\bar{3}m$ $\frac{5}{8}\frac{5}{8}\frac{5}{8}$	$\frac{1}{2}\frac{1}{2}1$(6)	
$C(S)$	$Ia\bar{3}d$-$Ia\bar{3}$	5	9	16*c* .3. $x_1x_1x_1$	$\bar{x}_1\bar{x}_1\bar{x}_1(1)$; $x_1, \bar{x}_1, \frac{1}{2}-x_1(3)$	$x_1 \approx 0{\cdot}1$
S	$Ia\bar{3}d$-$I\bar{4}3d$	5	11	12*a* $\bar{4}$..$\frac{3}{8}0\frac{1}{4}$	$x_1x_1x_1(4)$	$x_1 \approx 0{\cdot}2$
				16*c* .3. $x_1x_1x_1$	$\frac{3}{8}0\frac{1}{4}(3)$	
Y	$I4_132$-$P4_332$	6	9	4*a* .32 $\frac{1}{8}\frac{1}{8}\frac{1}{8}$	$\frac{\bar{1}}{8}\frac{3}{8}\frac{\bar{1}}{8}(6)$	
$C(Y)$	$I4_132$-$P4_332$	6	13	4*a* .32 $\frac{1}{8}\frac{1}{8}\frac{1}{8}$	$-\frac{1}{2}+x_1, \frac{1}{2}-x_1, 1-x_1(6)$	$x_1 \approx 0{\cdot}5$
				8*c* .3. $x_1x_1x_1$	$\frac{3}{8}\frac{7}{8}\frac{5}{8}(3)$	
$HS1$	$P6_222$-$P6_122(2c)$	7	7	6*b* ..2 $x_1, 2x_1, \frac{1}{4}$	$x_2, 1+y_2, z_2(2)$; $y_2, 1-x_2+y_2, -\frac{1}{6}+z_2(2)$	$x_1 \approx 0{\cdot}4$; $x_2 \approx 0{\cdot}25$;
				12*c* 1 $x_2y_2z_2$	$x_1, 2x_1-1, \frac{1}{4}(1)$; $1-x_1, x_1, \frac{5}{12}(1)$	$y_2 \approx 0$; $z_2 \approx 0{\cdot}3$
$HS2$	$P6_222$-$P3_212$	8	4	3*a* ..2 $x_1\bar{x}_1\frac{2}{3}$	$x_2, 2x_2, \frac{5}{6}(2)$	$x_1 \approx -0{\cdot}1$;
				3*b* ..2 $x_2\bar{x}_2\frac{1}{6}$	$2\bar{x}_1, \bar{x}_1, 0(2)$; $x_2, -1+2x_2, \frac{\bar{1}}{6}(2)$	$x_2 \approx 0{\cdot}25$
CLP	$P4_2/mcm$-$P4_2/mmc(v)$	9	3	2*a* *mmm*. 000	$00\frac{1}{2}(2)$; 100(2)	
tD	$P4_2/nnm$-$I4_1/amd$	10	3	4*a* $\bar{4}m2$ 000	$0\frac{1}{2}\frac{1}{4}(4)$	
$oCLP$	$Pccm$-$Cccm$	14	3	4*c* ..2/*m* 000	$00\frac{1}{2}(2)$; $\frac{1}{2}\frac{\bar{1}}{2}0(2)$	
oDa	$Pnnn$-$Fddd$	15	3	8*a* 222 000	$\frac{1}{4}\frac{1}{4}\frac{1}{4}(4)$	
oDb	$Cmma$-$Imma$	16	3	4*e* *mm*2 $0\frac{1}{4}z_1$	$\frac{1}{2}, \frac{1}{4}, \frac{1}{2}-z_1(2)$; $0\frac{3}{4}\bar{z}_1(2)$	$z_1 \approx 0{\cdot}1$
H	$P6_3/mmc$-$P\bar{6}m2$	22	3	1*a* $\bar{6}m2$ 000	$\frac{1}{3}\frac{2}{3}0(3)$	
				1*c* $\bar{6}m2$ $\frac{1}{3}\frac{2}{3}0$	000(3); $\frac{1}{3}\frac{2}{3}1(2)$	
$MC1$	$P6_3/mcm$-$P\bar{6}2m$	22	7	1*a* $\bar{6}2m$ 000	$x_100(3)$	$x_1 \approx x_2 \approx -0{\cdot}3$
				2*d* $\bar{6}$.. $\frac{1}{3}\frac{2}{3}\frac{1}{2}$	$\bar{x}_2\bar{x}_2\frac{1}{2}(3)$	
				3*f* *m*2*m* x_100	000(1); $x_20\frac{1}{2}(2)$	
				3*g* *m*2*m* $x_20\frac{1}{2}$	$\frac{\bar{1}}{3}\frac{1}{3}\frac{1}{2}(2)$; $x_100(2)$	
$C(H)$	$P6_3/mmc$-$P\bar{6}m2$	22	7	1*a* $\bar{6}m2$ 000	$\frac{2}{3}\frac{1}{3}\frac{1}{2}(6)$	
				1*d* $\bar{6}m2$ $\frac{1}{3}\frac{2}{3}\frac{1}{2}$	$\frac{2}{3}\frac{1}{3}\frac{1}{2}(3)$	
				1*f* $\bar{6}m2$ $\frac{2}{3}\frac{1}{3}\frac{1}{2}$	000(6); $\frac{1}{3}\frac{2}{3}\frac{1}{2}(3)$	
$R3$	$P6/mcc$-$P6/m$	23	13	1*a* 6/*m*.. 000	$x_1y_10(6)$	$x_1 \approx 0{\cdot}4$;
				2*c* $\bar{6}$.. $\frac{1}{3}\frac{2}{3}0$	$x_1-y_1, x_1, 0(3)$	$y_1 \approx 0{\cdot}1$
				6*j* *m*.. x_1y_10	000(1); $\frac{2}{3}\frac{1}{3}0(1)$; $1-x_1, \bar{y}_1, 0(1)$; $x_1y_11(2)$	
$MC2$	$P6/mcc$-$P6/m$	23	13	1*a* 6/*m*.. 000	$x_1y_10(6)$	$x_1 \approx x_2 \approx 0{\cdot}4$;
				2*c* $\bar{6}$.. $\frac{1}{3}\frac{2}{3}0$	$x_1-y_1, x_1, 0(3)$	$y_1 \approx y_2 \approx 0{\cdot}1$
				6*j* *m*.. x_1y_10	000(1); $\frac{2}{3}\frac{1}{3}0(1)$; $x_2y_2\frac{1}{2}(2)$	
				6*k* *m*.. $x_2y_2\frac{1}{2}$	$1-x_2, \bar{y}_2, \frac{1}{2}(1)$; $x_1y_10(2)$	
$MC3$	$P6/mcc$-$P6/m$	23	13	1*a* 6/*m*.. 000	$x_1y_10(6)$	$x_1 \approx x_2 \approx 0{\cdot}4$
				2*d* $\bar{6}$.. $\frac{1}{3}\frac{2}{3}\frac{1}{2}$	$x_2-y_2, x_2, \frac{1}{2}(3)$	$y_1 \approx y_2 \approx 0{\cdot}1$
				6*j* *m*.. x_1y_10	000(1); $1-x_1, \bar{y}_1, 0(1)$; $x_2y_2\frac{1}{2}(2)$	
				6*k* *m*.. $x_2y_2\frac{1}{2}$	$\frac{2}{3}\frac{1}{3}\frac{1}{2}(1)$; $x_1y_10(2)$	
$MC4$	$P6/mcc$-$P6/m$	23	13	1*b* 6/*m*.. $00\frac{1}{2}$	$x_2y_2\frac{1}{2}(6)$	$x_1 \approx x_2 \approx 0{\cdot}4$
				2*c* $\bar{6}$.. $\frac{1}{3}\frac{2}{3}0$	$x_1-y_1, x_1, 0(3)$	$y_1 \approx y_2 \approx 0{\cdot}1$
				6*j* *m*.. x_1y_10	$\frac{2}{3}\frac{1}{3}0(1)$; $1-x_1, \bar{y}_1, 0(1)$; $x_2y_2\frac{1}{2}(2)$	
				6*k* *m*.. $x_2y_2\frac{1}{2}$	$00\frac{1}{2}(1)$; $x_1y_10(2)$	
$C(R3)$	$P6/mcc$-$P6/m$	23	37	1*a* 6/*m*.. 000	$x_1y_1\frac{1}{2}(12)$	$x_1 \approx x_2 \approx 0{\cdot}4$;
				2*c* $\bar{6}$.. $\frac{1}{3}\frac{2}{3}0$	$x_1-y_1, x_1, \frac{1}{2}(6)$	$y_1 \approx 0{\cdot}1$;
				3*f* 2/*m*.. $\frac{1}{2}00$	$x_1y_1\frac{1}{2}(4)$	$y_2 \approx 0{\cdot}3$
				6*k* *m*.. $x_1y_1\frac{1}{2}$	000(2); $\frac{2}{3}\frac{1}{3}0(2)$; $\frac{1}{2}00(2)$; $x_2y_2\frac{1}{2}(1)$;	
					$y_2, -x_2+y_2, \frac{1}{2}(1)$; $1-y_2, x_2-y_2, \frac{1}{2}(1)$	
				6*k* *m*.. $x_2y_2\frac{1}{2}$	$x_1y_1\frac{1}{2}(1)$; $x_1-y_1, x_1, \frac{1}{2}(1)$;	
					$1-x_1+y_1, 1-x_1, \frac{1}{2}(1)$	
tP	$I4/mmm$-$P4/mmm$	24	3	1*a* 4/*mmm* 000	001(2); 100(4)	
$MC5$	$P4_2/mcm$-$Cmmm$	24	5	4*g* 2*mm* x_100	$\bar{x}_100(1)$; $x_20\frac{1}{2}(2)$	$x_1 \approx x_2 \approx 0{\cdot}25$
				4*h* 2*mm* $x_20\frac{1}{2}$	$x_100(2)$; $1-x_2, 0, \frac{1}{2}(1)$; $x_2\frac{1}{2}\frac{1}{2}(2)$	
$tC(P)$	$I4/mmm$-$P4/mmm$	24	9	1*a* 4/*mmm* 000	$\frac{1}{2}\frac{1}{2}0(4)$; $0\frac{1}{2}\frac{1}{2}(8)$	
				1*c* 4/*mmm* $\frac{1}{2}\frac{1}{2}0$	000(4)	
				2*e* *mmm*. $0\frac{1}{2}\frac{1}{2}$	000(4)	

Table 1 (*cont.*)

Minimal surface	G–H	Case	Genus	Labyrinth graph in H: Vertices	Adjacent vertices	Parameters
*R*2	*I*4/*mcm*–*P*4/*mbm*	25	9	2*a* 4/*m*.. 000 4*g* *m*.2*m* $x_1, \frac{1}{2}+x_1, 0$	$\frac{1}{2}-x_1, x_1, 0(4)$ $\frac{1}{2}\frac{1}{2}0(2)$; $1-x_1, \frac{3}{2}-x_1, 0(1)$; $x_1, \frac{1}{2}+x_1, 1(2)$	$x_1 \approx 0{\cdot}4$
*MC*6	*I*4/*mcm*–*P*4/*mbm*	25	9	2*a* 4/*m*.. 000 4*g* *m*.2*m* $x_1, \frac{1}{2}+x_1, 0$ 4*h* *m*.2*m* $x_2, \frac{1}{2}+x_2, \frac{1}{2}$	$\frac{1}{2}-x_1, x_1, 0(4)$ $\frac{1}{2}\frac{1}{2}0(2)$; $x_2, \frac{1}{2}+x_2, \frac{1}{2}(2)$ $x_1, \frac{1}{2}+x_1, 0(2)$; $1-x_2, \frac{3}{2}-x_2, \frac{1}{2}(1)$	$x_1 \approx x_2 \approx 0{\cdot}4$
*MC*7	*P*4/*mcc*–*P*4/*m*	25	9	1*b* 4/*m*.. $00\frac{1}{2}$ 1*c* 4/*m*.. $\frac{1}{2}\frac{1}{2}0$ 4*j* *m*.. x_1y_10 4*k* *m*.. $x_2y_2\frac{1}{2}$	$x_2y_2\frac{1}{2}(4)$ $x_1y_10(4)$ $\frac{1}{2}\frac{1}{2}0(1)$; $\bar{x}_1, 1-y_1, 0(1)$; $x_2y_2\frac{1}{2}(2)$ $00\frac{1}{2}(1)$; $x_1y_10(2)$	$x_1 \approx x_2 \approx 0{\cdot}1$; $y_1 \approx y_2 \approx 0{\cdot}4$
C(*R*2)	*I*4/*mcm*–*P*4/*mbm*	25	25	2*a* 4/*m*.. 000 2*d* *m*.*mm* $0\frac{1}{2}0$ 4*h* *m*.2*m* $x_1, \frac{1}{2}+x_1, \frac{1}{2}$ 4*h* *m*.2*m* $x_2, \frac{1}{2}+x_2, \frac{1}{2}$	$\bar{x}_1, \frac{1}{2}-x_1, \frac{1}{2}(8)$ $x_1, \frac{1}{2}+x_1, \frac{1}{2}(4)$ $\frac{1}{2}\frac{1}{2}0(4)$; $0\frac{1}{2}0(2)$; $x_2, \frac{1}{2}+x_2, \frac{1}{2}(1)$; $\frac{1}{2}-x_2, x_2, \frac{1}{2}(2)$ $x_1, \frac{1}{2}+x_1, \frac{1}{2}(1)$; $\frac{1}{2}-x_1, 1+x_1, \frac{1}{2}(2)$	$x_1 \approx 0{\cdot}1$; $x_2 \approx 0{\cdot}4$
oPb	*Fmmm*–*Cmmm*	26	3	2*b* *mmm* $\frac{1}{2}00$	$\frac{1}{2}01(2)$; $0\frac{1}{2}0(4)$	
*oMC*5	*Pccm*–*P*2/*m*	26	5	2*m* *m* x_1y_10 2*n* *m* $x_2y_2\frac{1}{2}$	$\bar{x}_1\bar{y}_10(1)$; $x_2y_2\frac{1}{2}(2)$ $x_1y_10(2)$; $1-x_2, 1-y_2, \frac{1}{2}(1)$; $\bar{x}_2, 1-y_2, \frac{1}{2}(1)$; $1-x_2, \bar{y}_2, \frac{1}{2}(1)$	$x_1 \approx x_2 \approx 0{\cdot}25$; $y_1 \approx y_2 \approx 0{\cdot}25$
oC(*P*)	*Fmmm*–*Cmmm*	26	9	2*a* *mmm* 000 2*b* *mmm* $\frac{1}{2}00$ 4*f* ..2/*m* $\frac{1}{4}\frac{1}{4}\frac{1}{2}$	$\frac{1}{2}00(2)$; $0\frac{1}{2}0(2)$ $000(2)$; $\frac{1}{2}\frac{1}{2}0(2)$; $\frac{1}{4}\frac{1}{4}\frac{1}{2}(8)$ $\frac{1}{2}00(4)$	
PT	*Fmmm*–*Cmmm*	26	5	2*b* *mmm* $\frac{1}{2}00$ 4*j* *m*2*m* $0y_1\frac{1}{2}$	$\bar{\frac{1}{2}}00(2)$; $\frac{1}{2}, \frac{1}{2}-y_1, \frac{1}{2}(4)$ $\frac{1}{2}00(2)$; $0y_1\frac{1}{2}(2)$	$y_1 \approx 0{\cdot}4$
*HS*3	$P6_222$–$P6_422(2c)$	27	7	3*a* 222 000 6*f* 2.. $\frac{1}{2}0z_1$	$0, \frac{1}{2}, \frac{1}{3}-z_1(4)$ $000(2)$; $\frac{1}{2}, 0, 1-z_1(1)$	$z_1 \approx 0{\cdot}3$
*ST*1	$P6_222$–$P6_422(2c)$	27	7	3*d* 222 $\frac{1}{2}0\frac{1}{2}$ 6*f* 2.. $\frac{1}{2}0z_1$	$\bar{\frac{1}{2}}0\frac{1}{2}(2)$; $\frac{1}{2}0z_1(2)$ $\frac{1}{2}0\frac{1}{2}(1)$; $\frac{1}{2}, \frac{1}{2}, \frac{2}{3}-z_1(2)$	$z_1 \approx 0{\cdot}3$
rPD	$R\bar{3}m$–$R\bar{3}m(2c)$	28	3	6*c* 3*m* $00z_1$	$00\bar{z}_1(1)$; $\frac{1}{3}, \frac{2}{3}, \frac{1}{3}-z_1(3)$	$z_1 \approx 0{\cdot}15$
*BC*1	$P6_322$–$P6_3$	31	9	2*a* 3.. $00z_1$ 2*b* 3.. $\frac{1}{3}\frac{2}{3}z_2$ 2*b* 3.. $\frac{1}{3}\frac{2}{3}z_3$ 6*c* 1 $x_4y_4z_4$ 6*c* 1 $x_5y_5z_5$	$x_5y_5z_5(3)$ $\frac{1}{3}\frac{2}{3}z_3(1)$; $x_4-y_4, x_4, \frac{1}{2}+z_4(3)$ $\frac{1}{3}\frac{2}{3}z_2(1)$; $\bar{y}_5, x_5-y_5, z_5(3)$ $\frac{2}{3}, \frac{1}{3}, -\frac{1}{2}+z_2(1)$; $x_5y_5z_5(1)$ $00z_1(1)$; $\frac{1}{3}\frac{2}{3}z_3(1)$; $x_4y_4z_4(1)$	$z_1 \approx z_3 \approx z_5 \approx 0{\cdot}4$; $z_2 \approx 0{\cdot}6$; $z_4 \approx 0{\cdot}1$; $x_4 \approx x_5 \approx 0{\cdot}3$; $y_4 \approx y_5 \approx 0$
*BC*2	$P4_2/nnm$–$P4_2nm$	32	7	2*a* 2.*mm* $00z_1$ 2*a* 2.*mm* $00z_2$	$00z_2(1)$; $\frac{1}{2}, \frac{1}{2}, -\frac{1}{2}+z_2(2)$ $00z_1(1)$; $\frac{1}{2}, \bar{\frac{1}{2}}, \frac{1}{2}+z_1(2)$; $10z_2(4)$	$z_1 \approx 0{\cdot}1$ $z_2 \approx 0{\cdot}4$
*ST*2	$P4_2/nbc$–$P4_2/n$	32	7	4*f* 2.. $00z_1$	$0, 0, 1-z_1(1)$; $\frac{1}{2}, \frac{1}{2}, \frac{1}{2}-z_1(2)$; $10z_1(2)$	$z_1 \approx 0{\cdot}4$
*BC*3	*I*422–*I*4	33	6	2*a* 4.. $00z_1$ 2*a* 4.. $00z_2$ 8*c* 1 $x_3y_3z_3$	$00z_2(1)$; $x_3y_3z_3(4)$ $00z_1(1)$; $10z_2(4)$; $\frac{1}{2}-x_3, \frac{1}{2}-y_3, \frac{1}{2}+z_3(4)$ $00z_1(1)$; $\frac{1}{2}, \frac{1}{2}, -\frac{1}{2}+z_2(1)$	$z_1 \approx 0{\cdot}1$; $z_2 \approx 0{\cdot}4$; $x_3 \approx 0{\cdot}1$; $y_3 \approx 0{\cdot}4$; $z_3 \approx 0$
C(±*Y*)	$Ia\bar{3}$–$Pa\bar{3}$	48	13	4*b* .$\bar{3}$. $\frac{1}{2}\frac{1}{2}\frac{1}{2}$ 8*c* .3. $x_1x_1x_1$	$\frac{1}{2}-x_1, \frac{1}{2}+x_1, x_1(6)$ $0\frac{1}{2}0(3)$	$x_1 \approx 0{\cdot}1$
±*Y*	$Ia\bar{3}$–$Pa\bar{3}$	48	21	8*c* .3. $x_1x_1x_1$	$\bar{x}_1\bar{x}_1\bar{x}_1(1)$; $x_1, \frac{1}{2}-x_1, \frac{1}{2}+x_1(3)$; $x_1, \frac{1}{2}-x_1, -\frac{1}{2}+x_1(3)$	$x_1 \approx 0{\cdot}1$
*Y**	$Ia\bar{3}d$–$I4_132$	—	3	8*a* .32 $\frac{1}{8}\frac{1}{8}\frac{1}{8}$	$\frac{3}{8}\frac{1}{8}\bar{\frac{1}{8}}(3)$	
oPa	*Immm*–*Pmmm*	—	3	1*a* *mmm* 000	100(2); 010(2); 001(2)	

by

$$g = 1 - \chi/2. \qquad (4)$$

The Euler characteristic may be derived in a simple way by dividing the surface into tiles. If f, e and v are the numbers of faces (tiles), edges and vertices, respectively, of such an arbitrary tiling

$$\chi = f - e + v \qquad (5)$$

holds. In the case of a three-periodic surface, the tiling has to be compatible with the translations of the surface. Then the faces, edges and vertices may either be counted per unit cell or for the surface embedded in T^3.

In the case of a minimal balance surface generated from disc-like surface patches spanned by skew polygons in a set of three-dimensionally connected twofold axes (Fischer & Koch, 1987; Koch & Fischer, 1988), these patches are symmetrically equivalent and may directly be used as tiles. Then f, e and v are the numbers of skew polygons, of (straight) edges and of vertices, respectively, referred to a primitive unit

cell of H. If e_p is the number of edges of one such polygon, and v_i is the multiplicity of the ith kind of symmetrically equivalent vertex (referred to a primitive unit cell of H), (5) may be rewritten as

$$\chi = f(1 - e_p/2) + \sum_i v_i. \qquad (6)$$

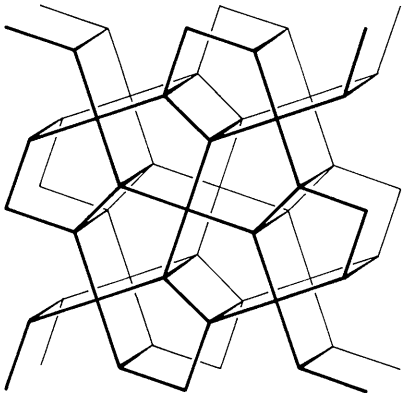

(a)

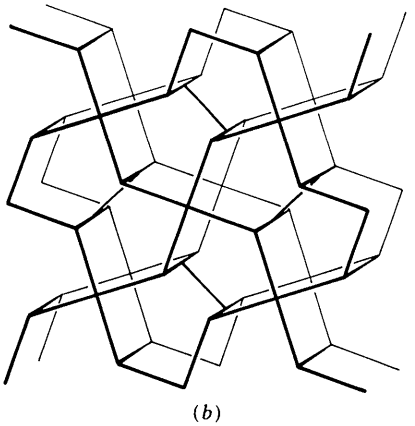

(b)

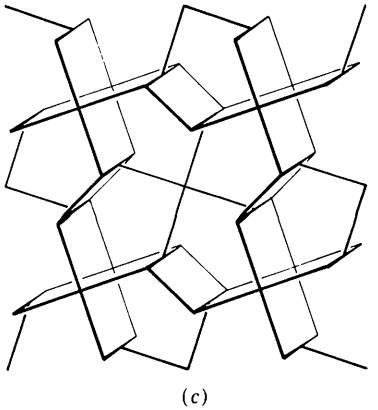

(c)

Fig. 1. Relationship between the labyrinth graphs of (*a*) an *R*2 surface, (*b*) an *MC*6 surface and (*c*) an *MC*7 surface. The graphs are projected onto the *ab* plane. In each case that part of one labyrinth graph is shown which corresponds to four unit cells of *H*.

If the minimal balance surface consists of catenoid-like surface patches spanned between plane parallel nets of twofold axes (Koch & Fischer, 1988), the catenoids cannot be used as tiles. In this case, however, one disc-like tile may be produced from each catenoid by cutting it up between two vertices. By this, one additional edge per catenoid is generated. If f_N, e_N and v_N are the numbers of faces (polygons), edges, and vertices, respectively, counted for all nets of twofold axes per unit cell, (5) may be rewritten as

$$\chi = v_N - e_N. \qquad (7)$$

From this a still simpler formula may be derived by making use of the relation

$$f_N - e_N + v_N = 0. \qquad (8)$$

As each catenoid is bounded by two polygons from the nets, combination of (4), (7) and (8) leads to

$$g = k + 1, \qquad (9)$$

where k is the number of catenoids per primitive unit cell of H.

In a similar way formulae have been derived for minimal balance surfaces built up from multiple catenoids (Koch & Fischer, 1989*a*; Karcher, 1988*), branched catenoids (Fischer & Koch, 1989*a*†) and catenoids with spout-like attachments (Koch & Fischer, 1989*b*). k means the number of surface patches per primitive unit cell of H in all cases. Then

$$g = km + 1 \qquad (10)$$

holds if the surface patch is a multiple catenoid made up of m catenoids,

$$g = k(1 + b)/2 + 1 \qquad (11)$$

if it is a branched catenoid with b branches at one end, and

$$g = ks + 1 \qquad (12)$$

if it is a catenoid with s spout-like attachments. Equation (9) also holds for minimal balance surfaces of which the surface patches are infinite strips (Fischer & Koch, 1989*b*). Then k is understood as the number of original catenoids per unit cell that have been united to the infinite rows.

The last four entries of Table 1 contain minimal balance surfaces that are either spanned by non-intersecting twofold axes [^+Y, (Fischer & Koch, 1987) and $C(^\pm Y)$ (Koch & Fischer, 1988)] or only fixed at (roto)inversion centres [Y^* or gyroid surface (Fischer & Koch, 1987; Schoen, 1970) and *oPa* (Karcher, 1988)]. In these cases disc-like surface patches may be used which are partly or totally bounded by curved lines, *e.g.* geodesics.

* These kinds of minimal surfaces have been derived simultaneously and independently by Karcher (1988) and by the authors.

† Table 1 of this paper contains a misprint: Last column, second row should read $2(2x, x, 0)$ instead of $2(2x, x, z)$.

The genus calculated from a labyrinth graph has been confirmed in this way in each case. A tabulation of the tilings used will not be given here, however, because of the close relationship to the surface patches described [except for type $C(^{\pm}Y)$] in the corresponding papers cited above. The surface patch of a $C(^{\pm}Y)$ surface resembles that of a $^{\pm}Y$ surface: it also is a skew 18-gon with symmetry $.\bar{3}.$ and alternately one straight and two curved edges. The straight edges and the vertices at their end points are the same in both cases, but the curved edges and their common vertices differ. With $x_1 \simeq 1/12$, a surface patch of a $C(^{\pm}Y)$ surface has the following vertices: $0, 0, \frac{1}{4}$; $\frac{1}{2}, 0, \frac{1}{4}$; $\frac{1}{2}+x_1, x_1, \frac{1}{2}-x_1$; $\frac{1}{2}, \frac{1}{4}, \frac{1}{2}$; $\frac{1}{2}, \frac{1}{4}, 0$; $\frac{1}{2}-x_1, x_1, \bar{x}_1$; $\frac{1}{4}, 0, 0$; $\frac{1}{4}, \frac{1}{2}, 0$; $\frac{1}{2}-x_1, \frac{1}{2}+x_1, x_1$; $\frac{1}{2}, \frac{1}{2}, \frac{1}{4}$; $0, \frac{1}{2}, \frac{1}{4}$; $\bar{x}_1, \frac{1}{2}-x_1, x_1$; $0, \frac{1}{4}, 0$; $0, \frac{1}{4}, \frac{1}{2}$; $x_1, \frac{1}{2}-x_1, \frac{1}{2}+x_1$; $\frac{1}{4}, \frac{1}{2}, \frac{1}{2}$; $\frac{1}{4}, 0, \frac{1}{2}$; $x_1, \bar{x}_1, \frac{1}{2}-x_1$. The close relationship between the two surfaces may be described also by another way of generation: A smaller surface patch (12-gon) is only spanned between the twofold axes within one eighth of the unit cell leaving free edges in between (*cf.* Fig. 2*a*). If this surface patch is continued by the twofold rotations, the resulting surface has pairs of triangular holes with symmetry $.\bar{3}.$ for the pair (those rotoinversion centres of $Ia\bar{3}$ that are kept in $Pa\bar{3}$). In a $^{\pm}Y$ surface each such pair of holes is closed by a catenoid-like patch (*cf.* Fig. 2*b*), whereas in a $C(^{\pm}Y)$ surface the two holes are spanned separately by two disc-like patches (*cf.* Fig. 2*c*). Though these completions of course affect the 12-gons near their free edges in different ways, most parts of them do not change visibly.

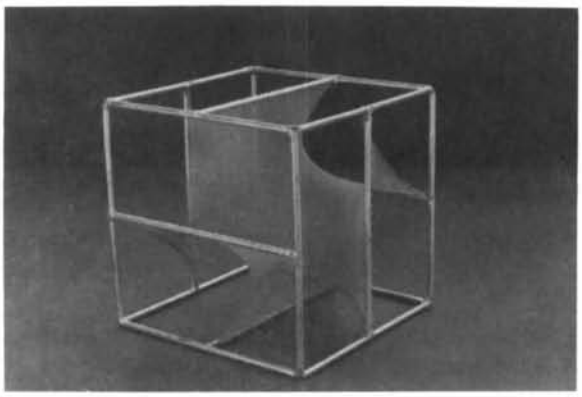

(*a*)

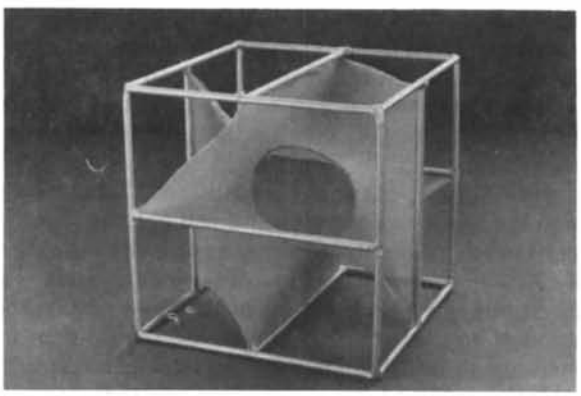

(*b*)

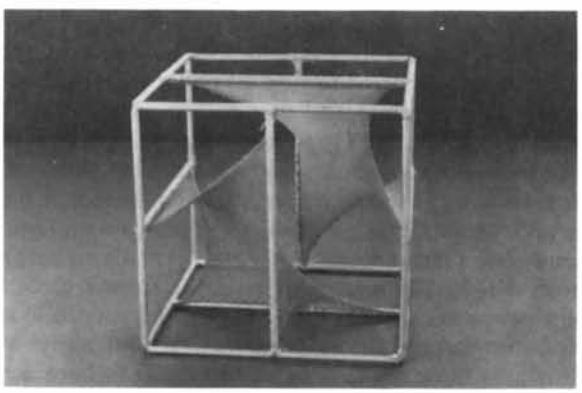

(*c*)

Fig. 2. Surface patches for $^{\pm}Y$ surfaces and for $C(^{\pm}Y)$ surfaces. The inherent symmetry is $Ia\bar{3}$–$Pa\bar{3}$ in both cases. Only one eighth of the unit cell of $Pa\bar{3}$ is shown: (*a*) 12-gon referring as well to a $^{\pm}Y$ surface as to a $C(^{\pm}Y)$ surface; (*b*) catenoid-like surface patch referring to a $^{\pm}Y$ surface; (*c*) pair of 6-gons referring to a $C(^{\pm}Y)$ surface.

A cubic unit cell may be orthorhombically deformed in two ways: (1) the orthorhombic and the cubic basis vectors coincide in their directions; only their lengths are different; (2) for one of the basis vectors the direction is kept; the other two change their directions (and their common angle), but they must be equal in length. Accordingly, two families of orthorhombically deformed *D* surfaces, *oDa* and *oDb*, have been observed. The derivation with the aid of twofold axes, however, yields only one family of orthorhombically deformed *P* surfaces, designated *oP* in previous papers and symbolized *oPb* in Table 1. Recently, Karcher (1988) has proved the existence of the second orthorhombic family *oPa*. Its inherent symmetry is *Immm*–*Pmmm* and the surfaces are only fixed by inversion centres.

The authors thank Dr S. T. Hyde, Canberra, and Dr S. Lidin, Lund, for helpful and enlightening discussions.

References

FISCHER, W. & KOCH, E. (1987). *Z. Kristallogr.* **179**, 31–52.
FISCHER, W. & KOCH, E. (1989*a*). *Acta Cryst.* A**45**, 166–169.
FISCHER, W. & KOCH, E. (1989*b*). *Acta Cryst.* A**45**, 485–490.
HYDE, S. T. (1989). *Z. Kristallogr.* In the press.
KARCHER, H. (1988). *The Triply Periodic Minimal Surfaces of Alan Schoen and their Constant-Mean-Curvature Companions.* Vorlesungsreihe no. 7. Sonderforschungsbereich 256. Institut für Angewandte Mathematik der Univ. Bonn, Federal Republic of Germany.

KOCH, E. & FISCHER, W. (1988). *Z. Kristallogr.* **183**, 129-152.
KOCH, E. & FISCHER, W. (1989*a*). *Acta Cryst.* A**45**, 169-174.
KOCH, E. & FISCHER, W. (1989*b*). *Acta Cryst.* A**45**, 558-563.
MACKAY, A. L. & KLINOWSKI, J. (1986). *Comput. Math. Appl.* **12B**, 803-824.
SCHOEN, A. H. (1970). *Infinite Periodic Minimal Surfaces Without Self-Intersections. NASA Tech. Note* No. D-5541.
WEEKS, J. R. (1985). *The Shape of Space: How to Visualize Surfaces and Three-Dimensional Manifolds. Monographs and Textbooks in Pure and Applied Mathematics*, Vol 96. New York, Basel: Marcel Dekker.

Acta Cryst. (1989). A**45**, 732-738

Theoretical Study of X-ray Diffraction in Homogeneously Bent Crystals – the Bragg Case

BY F. N. CHUKHOVSKII

Institute of Crystallography, Academy of Sciences of the USSR, Moscow 117333, *Leninsky Prospect* 59, *USSR*

AND C. MALGRANGE

Laboratoire de Minéralogie-Cristallographie, Universités Paris 6 *et* 7, *associé au CNRS*, 4 *Place Jussieu*, 75252 *Paris CEDEX* 05, *France*

(*Received* 23 *January* 1989; *accepted* 15 *June* 1989)

Abstract

X-ray dynamical diffraction in homogeneously bent crystals is studied theoretically in the Bragg case. The study starts from the Green function given previously by Chukhovskii, Gabrielyan & Petrashen' [*Acta Cryst.* (1978), A**34**, 610-620] as an inverse Laplace transform and which can be viewed as an integral over all incident plane waves. The integrand is developed by means of an asymptotic representation of parabolic cylinder functions. Integration by the stationary-phase method leads to the evidence of curved X-ray paths and, in the case of large values of strain gradient, to the creation of a new wave field. The intensity of the new wave field is shown to be a fraction $\exp(-2\pi|\nu|)$ of the incident beam where $|\nu|$ is the inverse of the strain gradient expressed in reduced units.

1. Introduction

The propagation of X-rays in distorted crystals has been widely studied since 1961 when Penning & Polder first published their geometrical-optics theory of propagation of wave fields. Their theory was based on an analogy with the propagation of light in inhomogeneous media. Then Kato (1963, 1964) developed a more rigorous theory using the Eikonal formulation and leading to the same results. Penning & Polder and Kato considered crystals distorted by a uniform strain gradient in the transmission or Laue case. Let us mention here that all theoretical works in this field have considered uniform strain gradients, that is distortions such that the second derivative of the projection of the displacement vector $\mathbf{u}(\mathbf{r})$ on the diffraction vector $\mathbf{h}$ with respect to the incident s_0 and reflected s_h directions is constant [$\partial^2(\mathbf{h}.\mathbf{u})/\partial s_0\,\partial s_h =$ constant]. Then Bonse (1964) generalized Penning & Polder's theory in order to apply it to the reflection or Bragg case and obtained hyperbolic trajectories for incident waves outside the domain of total reflection.

The three theories mentioned above are geometrical-optics theories and can only be valid for small strain gradients. Another approach to the study of X-ray propagation in distorted crystals was developed later, on the basis of the Green-Riemann-function method which takes into account diffraction phenomena and thus can be applied to large strain gradients. The Laue case was first treated by Petrashen' (1973), Chukhovskii (1974), Katagawa & Kato (1974), Petrashen' & Chukhovskii (1975, 1976), Chukhovskii & Petrashen' (1977). The Green function they obtained is a hypergeometric function which by itself does not provide any physical insight. Using asymptotic expansions, the authors were able to retrieve the results of geometrical theories in the case of small strain gradients and kinematical theory for extremely large strain gradients. Then Balibar, Chukhovskii & Malgrange (1983) expressed the hypergeometric function as an inverse Laplace transform from which they were able to evidence the creation of a new wave field at the apex of the hyperbolic ray path for strong strain gradients. Its intensity was shown to be a fraction $\exp(-2\pi/|\alpha_0|)$ (where α_0 is proportional to the strain gradient) of the intensity of the wave field before the apex of the trajectory. These results gave a theoretical basis to the computed results obtained previously by Balibar, Epelboin & Malgrange (1975).

The Bragg case was studied somewhat later. Petrashen' (1973) obtained the Riemann function as

0108-7673/89/100732-07$03.00